ELSEVIER

Nuclear Instruments and Methods in Physics Research B 141 (1998) 737–746

NIM B
Beam Interactions with Materials & Atoms

Track formation and dislocation loop interaction in spinel irradiated with swift heavy ions

S.J. Zinkle [a,*], V.A. Skuratov [b]

[a] *Metals and Ceremics Division, Oak Ridge National Laboratory, P.O. Box 2008, Oak Ridge, TN 37831-6376, USA*
[b] *Joint Institute for Nuclear Research, 141980 Dubna, Russian Federation*

Abstract

The microstructure of polycrystalline stoichiometric magnesium aluminate spinel ($MgAl_2O_4$) has been examined by cross-section electron microscopy following 430 MeV Kr^+ or 614 MeV Xe^+ ion irradiation near room temperature up to a fluence of 1.1×10^{16} ions/m^2. In addition, the microstructure was examined for two spinel specimens which had been preirradiated with either 2 MeV Al^+ ions or 3.6 MeV Fe^+ ions and subsequently irradiated with 430 MeV Kr^+ ions. The Al^+ and Fe^+ preirradiated specimens contained a high density (10^{21}–10^{23} m^{-3}) of interstitial dislocation loops with diameters between 5 and 30 nm prior to the swift heavy ion irradiation. Near-continuous latent ion tracks were observed in all of the specimens irradiated with swift heavy ions. The swift heavy ions also appeared to efficiently destroy pre-existing dislocation loops with diameters <5 nm, whereas larger loops remained intact following the swift heavy ion irradiation. The swift heavy ions caused structural disordering of the octahedral cautions, but did not appear to produce amorphous cores in the ion tracks. The disordered ion track diameters were ~2.0 and ~2.6 nm for the 430 MeV Kr and 614 MeV Xe ion irradiations, respectively. © 1998 Published by Elsevier Science B.V. All rights reserved.

PACS: 61.80.Jh
Keywords: Heavy ion irradiation; Spinel; Dislocation loops; Track formation

1. Introduction

Considerable interest has been generated in recent years in the phenomenon of latent track formation in insulators by swift heavy ions [1,2]. It is well established that continuous track formation by swift heavy ions is dependent on the material type, with typical values of the threshold electronic stopping powers $(dE/dx)_e$ ranging from ~1 to 20 keV/nm for insulators, and ~20 to 40 keV/nm for metals. However, the mechanism of defect production during irradiation in the electronic stopping power-dominant regime is still not understood. Several different theoretical models have been proposed to explain the track formation, including Coulombic explosion, thermal spikes, and self-trapped excitons [1–6]. Additional data on a wide range of materials are needed in or-

* Corresponding author. Tel.: +1 423 576 7220; fax: +1 423 574 0641; e-mail: zinklesj@ornl.gov.

0168-583X/98/$19.00 © 1998 Published by Elsevier Science B.V. All rights reserved.
PII S0168-583X(98)00078-0

der to test the validity of the available theoretical models.

Several studies have examined the susceptibility of radiolysis-resistant wide band gap insulators to track formation. Studies on Al_2O_3 observed significant amounts of disorder for $(dE/dx)_e = 24$–44 keV/nm, and the effective track diameter was variously estimated to be ~3.6 nm [7,8] and 2.0–5.2 nm [9] as $(dE/dx)_e$ increased from 24 to 44 keV/nm. However, it was uncertain whether the core of the ion track was amorphous vs. a disordered crystalline state in these studies [8,10]. Other work found that the electronic energy loss threshold for damage production in Al_2O_3 and MgO is 20 and 22 keV/nm, respectively, and that amorphization in the ion track core does not occur for $(dE/dx)_e$ up to 40 keV/nm [11]. Recently, Skuratov and coworkers noted that a sharp decrease in the luminescence intensity ratio of F vs. F^+ centers occurred in alumina irradiated with swift heavy ions above $(dE/dx)_e \sim 5$ keV/nm [12]. Several different swift heavy ion irradiation studies have been performed on magnetic insulators with the spinel crystal structure, including $MgFe_2O_4$, $NiFe_2O_4$ and $ZnFe_2O_4$ [10,13–16]. Continuous latent ion track amorphization was observed in $ZnFe_2O_4$ for $(dE/dx)_e = 26$ keV/nm, but not at 16 keV/nm. Evidence was also obtained for structural mixing of the octahedral Fe cations due to swift heavy ion irradiation [16]. Comparable swift heavy ion irradiation studies on $MgAl_2O_4$ spinel have not been reported.

The band gaps in $MgAl_2O_4$ [17] and Al_2O_3 [18] are both 9 eV, and many of the other key physical properties are comparable. Therefore, it might be expected that $MgAl_2O_4$ should exhibit behavior similar to that of Al_2O_3 during swift heavy ion irradiation. On the other hand, $MgAl_2O_4$ generally exhibits superior radiation resistance compared to alumina [19,20], and is more resistant to ion beam-induced amorphization [21,22]. One possible contributing reason for the superior radiation resistance of $MgAl_2O_4$ is that its interstitial migration energy is significantly lower than that of alumina (0.21 vs. 0.6 eV) [23]. It has also been noted that $MgAl_2O_4$ is more sensitive to moderate levels of ionizing radiation, which is presumably associated with ionization-induced diffusion effects [24–26]. One of the objectives of the present study was to determine whether the behavior of $MgAl_2O_4$ under swift heavy ion irradiation conditions was similar to previously reported results on alumina.

The second objective of the present study was to examine the interaction of swift heavy ions with dislocation loops and metallic precipitates in spinel. There have been several previous studies on the interaction between swift heavy ions and preexisting microstructural features [1,11,13,27,28]. For example, electrical resistivity studies noted a pronounced amount of radiation annealing at 5–10 K during swift heavy ion irradiation of predamaged Fe and Ni specimens [1,27]. Track formation in precipitates [13] and precipitate dissolution [11,28] has also been reported in ceramics irradiated with swift heavy ions.

2. Experimental procedure

The material for this study was polycrystalline (~30 μm grain diameter) stoichiometric magnesium aluminate spinel ($MgAl_2O_4$) which was produced by Ceredyne, Costa Mesa, CA [29]. The inversion parameters was estimated to be $i \sim 0.15$ by ALCHEMI (Atom Location by Channeling Enhanced MIcroanalysis) techniques [30]. Transmission electron microscope specimens with dimensions of 3 mm diameter by 0.5 mm thickness were cut from the sintered block and mechanically polished with 0.5 μm diamond paste. Several of these specimens were subsequently irradiated with either 3.6-MeV Fe ions at 50°C to a fluence of 1.2×10^{20} ions/m^2 or 2-MeV Al ions at 650°C to a fluence of 3.7×10^{21} ions/m^2 in the triple ion beam accelerator facility at Oak Ridge National Laboratory [31]. According to TRIM96 [32] calculations, these fluences produced peak displacement per atom (dpa) levels of ~6 and 100 dpa, respectively. The calculated ion range was ~1.4 μm for both irradiation conditions. The specimens were irradiated in a target holder that contained an array of nine specimens. Therefore, nearly identical irradiated specimens were available for examining the microstructure before and after the subsequent swift heavy ion irradiation. One each of the Al-

Table 1
Irradiation conditions for the spinel specimens (the swift heavy ion irradiations were performed near room temperature)

Sample number	Pre-irradiation condition	Swift heavy ion fluence
1	2 MeV Al, 650°C, 3.7×10^{21} m^{-2}	1.1×10^{16} ions/m^2 (430 MeV Kr)
2	3.6 MeV Fe, 50°C, 1.2×10^{20} m^{-2}	1.1×10^{16} ions/m^2 (430 MeV Kr)
3	–	1.1×10^{16} ions/m^2 (430 MeV Kr)
5	–	0.6×10^{16} ions/m^2 (614 MeV Xe)

and Fe-ion irradiated specimens was irradiated near room temperature with 430 MeV Kr^+ ions (5.1 MeV/amu) at the Dubna U-400 cyclotron facility. In addition, two spinel specimens which were not preirradiated with Al- or Fe-ions were irradiated near room temperature with 430 MeV Kr^+ and 614 MeV Xe^+ (4.6 MeV/amu) ions, respectively. Table 1 summarizes the irradiation matrix for this study.

The maximum swift heavy ion fluence of 1.1×10^{16} ions/m^2 (average track separation ~15 nm) was chosen to exclude ion track overlapping and thereby examine the effects associated with single ion tracks. The swift heavy ion flux was maintained at about 5×10^{12} ions/m^2 s during the irradiation. The calculated range for both of the swift heavy ion species in spinel is ~29 μm. The calculated electronic stopping power for the swift heavy ions in the near-surface region ($\leqslant 5$ μm depths) was 16 and 26 keV/nm for the 430 MeV Kr^+ and 614 MeV Xe^+ ions, respectively. The corresponding damage energy (nuclear stopping power minus the electronic stopping power of recoiling ions) was three orders of magnitude smaller. Assuming a sublattice-overaged displacement energy of 40 eV, the maximum dose produced by elastic collisions with the swift heavy ions was $\sim 1 \times 10^{-5}$ dpa for depths up to 15 μm, and $\sim 10^{-3}$ dpa in the peak damage region (~29 μm). Table 2 summarizes the calculated [32] irradiation parameters for the various ion beams used in this study.

Following irradiation, cross-section TEM specimens were prepared using standard [33] techniques of grinding, dimpling and ion milling. The microstructure was examined using either a Philips CM12 or CM200 transmission electron microscope operating at 120 and 200 kV, respectively.

3. Results

Nearly continuous ion tracks were observed in all of the specimens irradiated with swift heavy ions at depths up to 23 μm $(dE/dx)_e$ >13 keV/nm). Residual damage from the swift heavy ion irradiation was clearly visible even at low magnification. Examination at higher magnification revealed that defect clusters were formed along the periphery of the ion tracks. Fig. 1 shows an example of a medium-magnification bright field image of spinel irradiated with 430 MeV Kr ions. Weak beam dark field analysis performed at higher magnification showed that many of the defect

Table 2
Calculated irradiation parameters for the spinel specimens investigated in this study (the swift heavy ion parameters are valid for depths of 0–15 μm)

Ion type	$(dE/dx)_e$ (keV/nm)	Damage energy, S_d (keV/nm)	Damage level (dpa)
3.6 MeV Fe	$\leqslant 3.4$	0.1–0.6	1–6
2 MeV Al	$\leqslant 2.4$	0.04–0.28	30–100
430 MeV Kr	16	0.005–0.01	$0.5–1 \times 10^{-5}$
614 MeV Xe	27	0.01–0.03	$0.6–1.4 \times 10^{-5}$

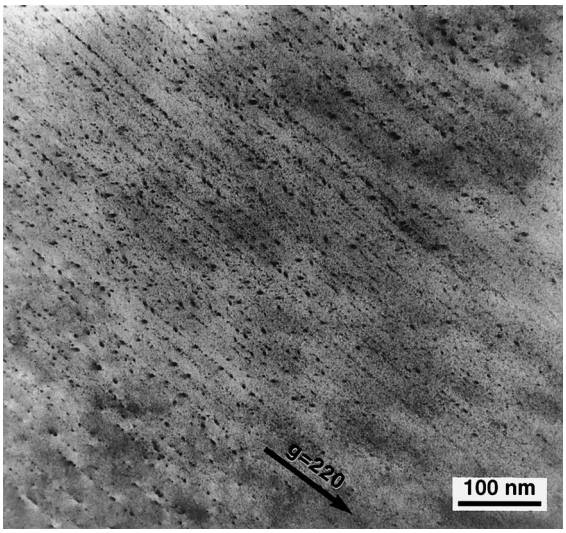

Fig. 1. Bright-field microstructure of spinel irradiated with 430 MeV Kr ions to a fluence of 1.1×10^{16} ions/m^2.

clusters were resolvable as small dislocation loops which formed on {1 1 1} habit planes. Similar types of interstitial dislocation loops have been observed in neutron or ion irradiated spinel [20,22,25]. However, the mechanism for the creation of the point defects is considerably different for the swift heavy ion irradiation, since the amount of displacement damage attributable to elastic collisions is only $\sim 10^{-5}$ dpa (Table 2). The loop nature (vacancy vs. interstitial) in the swift heavy ion irradiated specimens was not determined due to the small size of the loops.

The ion track diameter was measured by centered dark field imaging with a diffraction vector of $g = 222$. It was not possible to measure the ion track diameter in the cross-section specimens using high resolution lattice imaging techniques, since the large fraction of crystalline material above and below a given ion track obscures any disorder occurring in the ion track [34]. The $g = 222$ dark field imaging condition is convenient in spinel specimens containing a high amount of radiation damage because the near-zero electron structure factor provides relatively weak intensity and therefore, overlapping defect contrast effects are minimized. The octahedral cations provide the main contribution to the 222 electron structure factor in spinel (tetrahedral cations do not contribute and anions give a slight destructive contribution). Fig. 2 shows the ion track cores which were imaged in spinel irradiated with 430 MeV Kr ions. The measured diameter of the ion tracks was 2.0 ± 0.4 nm at depths from 0 to 15 μm. The corresponding ion track diameter for the 614 MeV Kr ions was 2.6 ± 0.4 nm at depths of ~10–15 μm. Discontinuous ion track damage consisting of discrete defects with sizes 4–12 nm was observed during $g = 222$ centered dark field imaging at depths <10 μm in the specimen irradiated with 614 MeV Kr ions. The presence of the dark-diffracting ion track cores in Fig. 2 indicates that the intensity associated with octahedral cation scattering in the ion tracks is less than in the unirradiated regions of the matrix. This could be associated with either amorphization or else pronounced structural disordering in the ion track region. Conventional high-magnification centered dark field imaging at diffraction vector values corresponding to the position of the first intensity maximum in amorphous spinel (~3.5 nm^{-1}) did not reveal any evidence of amorphous ion cores. Therefore, it is concluded that the ion track cores in the spinel specimens are structurally disordered (significant decrease in octahedrally coordinated cations), but they do not appear to be amorphous. Lattice imaging of plan view specimens will be performed to further investigate the ion track structure.

3.1. Examination of predamaged specimens

Based on TEM analysis of sibling specimens which were simultaneously irradiated in the 9-specimen target holder at ORNL, the 3.6 MeV Fe ion irradiation at 50°C produced an average interstitial dislocation loop diameter of ~5 nm and loop density $\sim 2 \times 10^{23}$ m^{-3} The loop parameters were nearly independent of depth over the Fe ion-irradiated region. The corresponding values for the spinel specimen irradiated with Al ions at 650°C were ~30 nm and $\sim 1 \times 10^{21}$/m^3 at a depth of ~0.6 μm. In this specimen, the loop diameter decreased and the loop density increased with increasing depth in the Al ion irradiated region [35]. Metallic aluminum precipitates were formed in the Al ion preirradiated specimens at depths

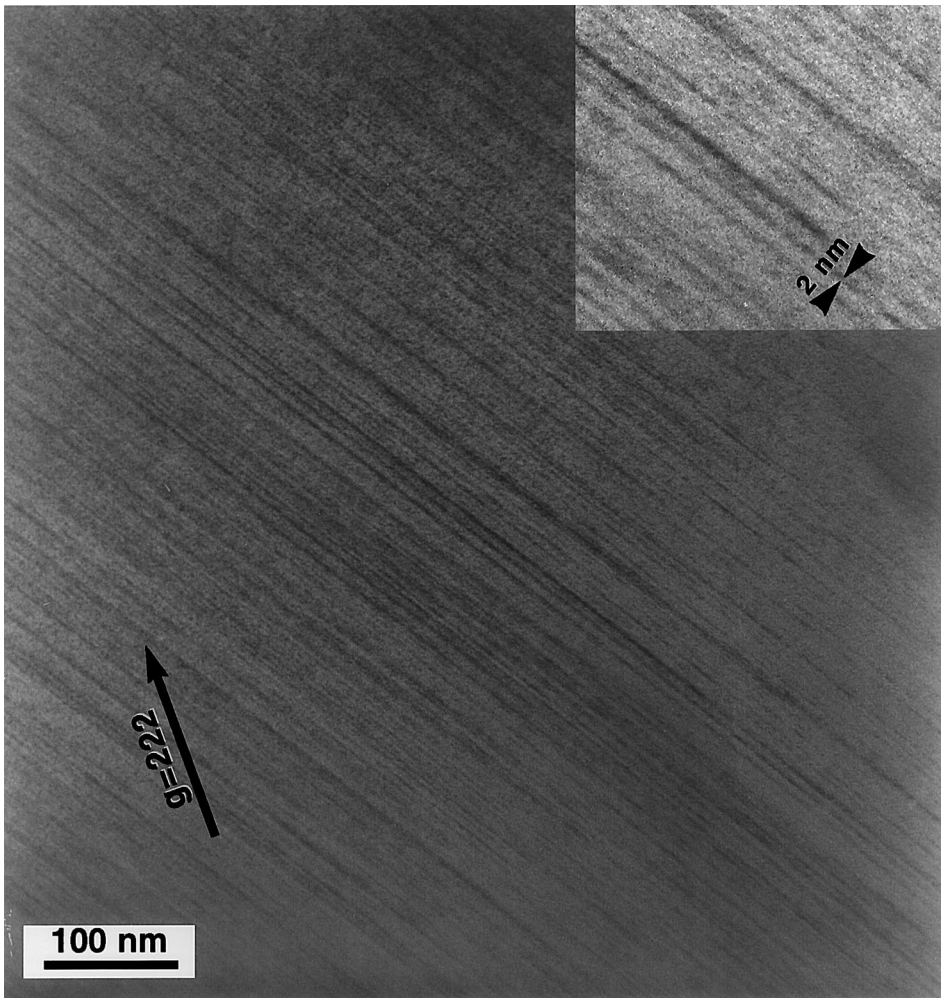

Fig. 2. Ion tracks in spinel irradiated with 430 MeV Kr ions to a fluence of 1.1×10^{16} ions/m^2, imaged using $g = 222$ centered dark field conditions. The inset shows the same region at higher magnification.

of ~1.3–1.8 μm, which corresponds to the Al implantation region [24,36]. The average precipitate density was $\sim 4 \times 10^{22}$ m^{-3} and the precipitate diameter ranged from 2 to 25 nm.

Fig. 3 shows the low-magnification cross-section microstructure of spinel that was preirradiated with 2 MeV Al ions and then irradiated with 430 MeV Kr ions. Faint traces of the ion tracks can be seen in the near-surface region and at depths greater than the Al ion range (1.8 μm). Fig. 4 shows the dislocation microstructure in the Al ion preirradiated region at higher magnification. There was no evidence for any change in the dislocation loop parameters compared to results obtained on specimens irradiated with 2 MeV Al ions only. The Burgers vectors of the dislocation loops were analyzed to be of the type a/4 ⟨1 1 0⟩ and the loop habit planes were determined to be predominantly {1 1 0} with a small fraction of loops lying on {1 1 1} or intermediate planes, in agreement with measurements made on specimens irradiated with 2 MeV Al ions only. A comparison of the Al participates in Al ion preirradiated specimens with and without swift heavy ion irradiation

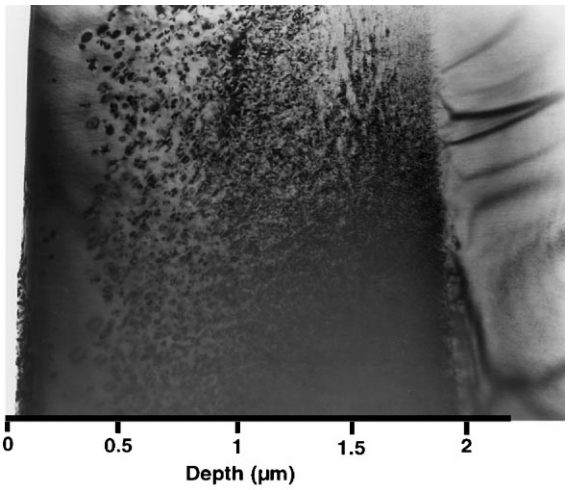

Fig. 3. Cross-section microstructure of a spinel specimen that was preirradiated with 2 MeV Al ions and then irradiated with 430 MeV Kr ions.

indicated that there was no significant change in the density or size distribution. Some evidence of ballistic dissolution was observed in a small fraction (<3%) of the Al precipitates with sizes <5 nm.

Following swift heavy ion irradiation, the low-magnification defect cluster contrast in the 3.6 MeV Fe ion preirradiated regions of the specimen was significantly weaker than in specimens irradiated with 3.6 MeV Fe ions alone. Quantitative analysis of the dislocation loop parameters in the 3.6 MeV Fe ion preirradiated region after swift heavy ion irradiation indicated that the loop size had decreased to ~4 nm and the loop density had increased to $\sim 4 \times 10^{25}$ m^{-3}. This slight refinement in the loop parameters suggests that the swift heavy ions have caused dissolution (and perhaps reformation) of some of the pre-existing dislocation loops. Fig. 5 shows an example of the weak beam microstructure in the 3.6 MeV Fe ion preirradiated region following 430 MeV Kr ion irradiation. Weak contrast associated with defect cluster formation along the periphery of the swift heavy ion track is visible in the photo.

One interesting observation was that the ion track damage was considerably less pronounced in the Al and Fe ion preirradiated regions compared to deeper regions which were only exposed to the swift heavy ions. Fig. 6 shows pronounced

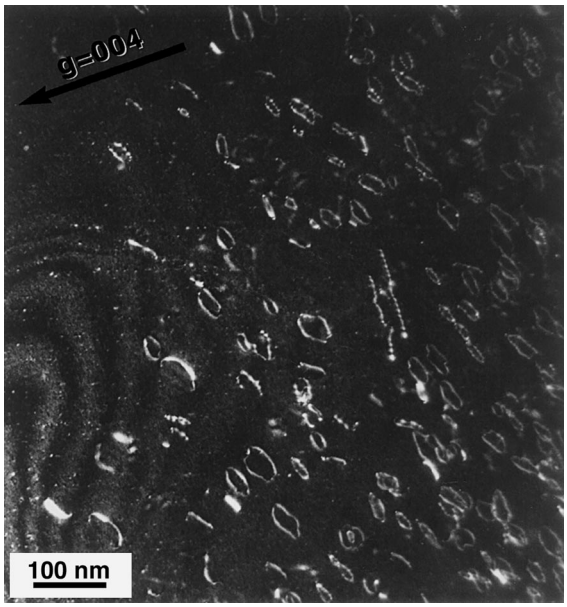

Fig. 4. Weak beam (g, $3g$), $g = 004$ microstructure in the 2 MeV Al ion preirradiated region of spinel following 430 MeV Kr ion irradiation. The beam direction is near [1 $\bar{1}$ 0].

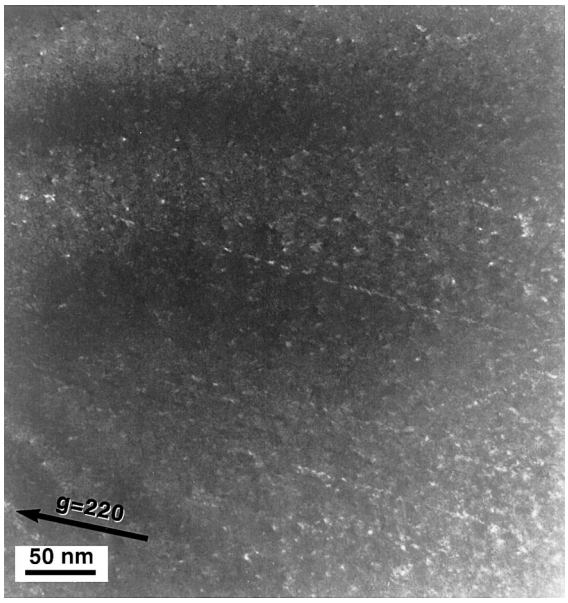

Fig. 5. Weak beam (g, $3g$), $g = 220$ microstructure in the 3.6 MeV Fe ion preirradiated region of spinel following 430 MeV Kr ion irradiation. The beam direction is near [1 $\bar{1}$ 0].

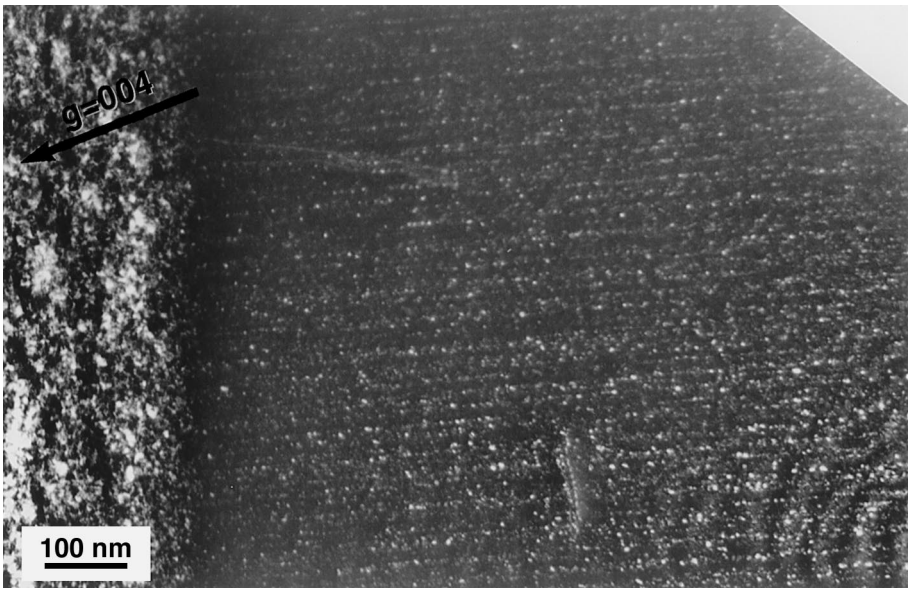

Fig. 6. Weak beam (g, $3g$), $g = 004$ microstructure beyond the end of range of the 2 MeV Al ion preirradiated region after 430 MeV Kr ion irradiation. The beam direction is near [1 $\bar{1}$ 0].

defect cluster formation along the swift heavy ion tracks in spinel in a region just beyond the end of the 2 MeV Al ion damage range. In contrast, Fig. 4 demonstrates that ion track damage was not visible in the Al ion preirradiated region in the same grain for the same imaging conditions. Imaging of the ion track using g = 222 diffraction vectors similarly indicated reduced ion track visibility in the Al and Fe ion preirradiated regions.

4. Discussion

The presence of nearly continuous tracks in $MgAl_2O_4$ with a core radius of ~1.0–1.3 nm for swift heavy ions with $(dE/dx)_e$ ~16–27 keV/nm is in general agreement with data obtained on Al_2O_3 [2,7–9], MgO [11] and magnetic spinel insulators [10,13–16], although somewhat larger track radii were reported in the previous studies on $MgFe_2O_4$ and $NiFe_2O_4$ magnetic spinels. Discontinuous tracks were observed in $ZnFe_2O_4$ spinel irradiated with $(dE/dx)_e$ ~20 keV/nm [14], and amorphization (6 nm track diameter) was reported to occur for $(dE/dx)_e$ ~23 keV/nm [16].

The core of the swift heavy ion track in $MgAl_2O_4$ does not appear to be amorphous for the electronic stopping powers investigated in this study, in agreement with previous results on Al_2O_3 and MgO irradiated up to $(dE/dx)_e$ ~40 keV/nm [11] but in disagreement with the results on $ZnFe_2O_4$ discussed in the previous paragraph. The observation of dark diffracting ion tracks in $MgAl_2O_4$ under $g = \langle 222 \rangle$ diffraction conditions (Fig. 2) suggests that the ion track core has become severely distorted from the normal spinel structure to a disordered structure with a significantly lower fraction of octahedral cations. Similar conclusions regarding octahedral cation disordering by swift heavy ions were previously reported for magnetic insulator spinels [16]. Cation randomization on octahedral and tetrahedral sites has also been previously reported for neutron-irradiated spinels [37,38]. No evidence for an amorphous track was observed by conventional high-magnification center dark field imaging. However, it should be noted that amorphous spinal can be easily recrystallized by the ionizing radiated associated with 100–200 keV electron beams [39]. Therefore, it is possible that amorphous ion tracks may

have been produced by the swift heavy ions, but were not observable by electron microscopy due to electron beam-stimulated recrystallization. Amorphization of spinel has been recently observed by cross-section TEM following 72 MeV I^+ ion irradiation at 300 K to fluences of 10^{18}–10^{20} ions/m^2 along the first $\frac{2}{3}$ of the ion track, where the electronic stopping power exceeded ~8 keV/nm [39]. In this unpublished study, partial amorphization was observed after 10^{18} ions/m^2, and complete amorphization occurred after 10^{20} ions/m^2. Further work is needed to determine if amorphization of $MgAl_2O_4$ occurs directly in the swift heavy ion track cores, or alternatively if overlapping ion tracks are necessary to induce amorphization.

The physical mechanism responsible for the suppression of swift heavy ion-produced defect cluster formation in regions predamaged by 3.6 MeV Fe ions or 2 MeV Al ions is uncertain. The ion track core imaged with $g = 222$ centered dark field conditions was also generally weaker in predamaged regions. The preirradiation would have caused some cation disordering in the spinel lattice (which could explain the relative weakness of the ion tracks using $g = 222$ imaging conditions in the predamaged regions), but it is not clear why cation disordering would inhibit defect cluster formation at the periphery of the swift ion track.

The destruction of pre-existing dislocation loops by the swift heavy ions appeared to occur if the loop size was comparable to the ion track size (loop diameter ~5 nm). The swift heavy ions did not appear to have any effect on the larger (~30 nm diameter) loops present in the 100 dpa Al-ion preirradiated specimen. Although differences in the Burgers vectors of the loops in the Al and Fe preirradiated specimens may play some role, the results appear to simply suggest that loops with sizes comparable or smaller than the swift heavy ion track are efficiently destroyed by the impinging ion. From geometric considerations, the interaction probability of the swift heavy ion with dislocation loops is $P \sim [1 - \exp - \sigma\phi t]$, where $\sigma = \pi/4(0.5\ d_{loop} + R_{ion})^2$ and ϕt is the fluence. The factor of 0.5 accounts for the cosine-squared average of projected loop diameters (d_{loop}) in order to account for the random loop orientation with respect to the swift heavy ion beam. The normalized probability of an ion track interacting with a dislocation loop (and causing its dissolution) is therefore strongly dependent on the ion track radius for small loop sizes. It is not clear a priori whether the observed ion track "core" radius (~1 nm) or the mean diffusion length for deposited energy, $\lambda \sim 4$ nm [40] is the more appropriate parameter to use for the ion beam interaction radius (R_{ion}). The calculated values of P for a fluence of 1.1×10^{16} ions/m^2 and a dislocation loop diameter of 5 nm are ~10% for $R_{ion} = 1$ nm and ~30% for $R_{ion} = 4$ nm. Since a significant fraction of the ~5 nm diameter loops in the Fe-preirradiated spinel specimen were apparently affected by subsequent swift heavy ion irradiation, this suggests that the effective interaction radius of the swift heavy ion beam with small dislocation loops is considerably larger than the disordered ion core radius. It is worth noting that all of the large loops in the spinel specimen preirradiated at 650°C with Al ions (~30 nm diameter) would have been struck by one or more swift heavy ions (i.e., the loop diameter is about twice as large as the average ion track spacing for the fluences used in this study).

The swift heavy ions appeared to be relatively inefficient regarding dissolution of aluminum precipitates with diameters 2–25 nm. Previous work has reported that ~30% of Na precipitates in MgO with an average diameter of 10 nm were dissolved following swift heavy ion irradiation to an order of magnitude higher fluence (2.2×10^{16} ions/m^2) than the present study [11,28]. The derived dissolution cross-section of ~10^{-18} m^2 at $(dE/dx)_e$ ~20 keV/nm for the Na precipitate study [28] is about an order of magnitude smaller than the dissolution cross-section for small dislocation loops estimated in the preceding paragraph. Therefore, fluences above ~10^{17} m^{-2} may be necessary in order to observe Al precipitate dissolution in $MgAl_2O_4$.

5. Conclusions

Swift heavy ion irradiation of $MgAl_2O_4$ with $(dE/dx)_e$ ~16–27 keV/nm produced continuous disordered ion tracks with a diameter of ~2.0–

2.6 nm. Significant disordering of the octahedral cations occurred within the ion track core, but the core was apparently not amorphous. It is possible that electron beam-stimulated recrystallization might prevent viewing of the amorphous core in an electron microscope. A significant concentration of small (3–5 nm diameter) dislocation loops were resolved among the defect cluster debris at the periphery of the swift heavy ion tracks. The defect cluster debris was significantly less pronounced in regions of the specimens which had been preirradiated with either 2 MeV Al or 3.6 MeV Fe ions. The swift heavy ion irradiation caused refinement of pre-existing dislocation loops with diameters <5 nm, but had no effect on large (~30 nm diameter) loops. The swift heavy ion dissolution cross-section for Al precipitates with diameters of 2–25 nm was apparently significantly smaller than the dissolution cross-section for small (~5 nm diameter) dislocation loops in $MgAl_2O_4$.

Acknowledgements

The authors thank J.W. Jones for the preparation of the cross-section TEM specimens, and I.M. Anderson for enlightening discussions on the spinel electron structure factor. This research was sponsored in part by the Office of Fusion Energy Sciences, US Department of Energy under contract DE-AC05-96OR22464 with Lockheed Martin Energy Research Corp.

References

[1] A. Dunlop, D. Lesueur, Mater. Sci. Forum 97–99 (1992) 553.
[2] M. Toulemonde, S. Bouffard, F. Studer, Nucl. Instr. and Meth. B 91 (1994) 108.
[3] R.L. Fleischer, P.B. Price, R.M. Wallner. Nuclear Tracks in Solids, Principles and Applications, University of California Press, Berkeley, 1975.
[4] G. Szenes, Nucl. Instr. and Meth. B 116 (1996) 141.
[5] N. Itoh, Nucl. Instr. and Meth. B 116 (1996) 33.
[6] A. Miotello, R. Kelly, Nucl. Instr. and Meth. B 122 (1997) 458.
[7] B. Canut et al., Nucl. Instr. and Meth. B 80/81 (1993) 1114.
[8] J.M. Marty et al., Nucl. Instr. and Meth. B 91 (1994) 274.
[9] B. Canut et al., Phys. Rev. B 51 (1995) 12194.
[10] F. Studer, M. Hervieu, J.M. Costantini, M. Toulemonde, Nucl. Instr. and Meth. B 122 (1997) 449.
[11] P.A. Thevenard, M. Beranger, B. Canut, S.M.M. Ramos, in: D.B. Poker et al. (Ed.), Ion-Solid Interactions for Materials Modification and Processing, MRS Symposium Proceedings, vol. 396, Materials Research Society, Pittsburgh, 1996, p. 127.
[12] V.A. Skuratov, S.M. Abu-AlAzm, V.A. Altynov, Mater. Sci. Forum 248–249 (1997) 399.
[13] M. Treilleux et al., Nucl. Instr. and Meth. B 32 (1988) 397.
[14] C. Houpert et al., Nucl. Instr. and Meth. B 32 (1988) 393.
[15] C. Houpert, D. Groult, F. Studer, M. Toulemonde, Radiat. Eff. Def. Solids 110 (1989) 189.
[16] F. Studer et al., Nucl. Instr. and Meth. B 82 (1993) 91.
[17] J.D. Woosley, C. Wood, E. Sonder, R.A. Weeks, Phys. Rev. B 22 (1980) 1065.
[18] B.D. Evans, J. Nucl. Mater. 219 (1995) 202.
[19] F.W. Clinard Jr., G.F. Hurley, L.W. Hobbs, J. Nucl. Mater. 108, 109 (1982) 655.
[20] C. Kinoshita et al., J. Nucl. Mater. 219 (1995) 143.
[21] S.X. Wang, L.M. Wang, R.C. Ewing, in: I.M. Robertson et al. (Eds.), Microstructure Evolution During Irradiation, MRS Symposium Proceedings, vol. 439, Materials Research Society, Pittsburgh, 1997, p. 619.
[22] S.J. Zinkle, G.P. Pells, J. Nucl. Mater. 253 (1998).
[23] S.J. Zinkle, L.L. Snead, Unpublished research presented at American Ceramics Society symposium on Fabrication and Properties of Ceramics for Fusion Energy and Other High Radiation Environments, 1997.
[24] S.J. Zinkle, Nucl. Instr. and Meth. B 91 (1994) 234.
[25] S.J. Zinkle, J. Nucl. Mater. 219 (1995) 113.
[26] S.J. Zinkle, in: I.M. Robertson et al. (Eds.), Microstructure Evolution During Irradiation, MRS Symposium Proceedings, vol. 439, Materials Research Society, Pittsburgh, 1997, p. 667.
[27] T. Iwata, A. Iwase, Nucl. Instr. and Meth. B 61 (1991) 436.
[28] M. Beranger et al., Phys. Rev. B 53 (1996) 14773.
[29] S.J. Zinkle, J. Am. Ceram. Soc. 72 (1989) 1343.
[30] I.M. Anderson, ORNL, 1996, unpublished research.
[31] M.B. Lewis et al., Nucl. Instr. and Meth. B 43 (1989) 243.
[32] J.F. Ziegler, J.P. Biersack, U. Littmark, The Stopping and Range of Ions in Solids, Pergamon Press, New York, 1985.
[33] S.J. Zinkle, C.P. Haltom, L.C. Jenkins, C.K.H. DuBose, J. Electron Microsc. Tech. 19 (1991) 452.
[34] M.L. Miller, R.C. Ewing, Ultramicrosopy 48 (1993) 203.
[35] S.J. Zinkle, in: R.E. Stoller, A.S. Kumar, D.S. Gelles (Eds.), 15th International Symposium on Effects of Radiation on Materials, ASTM STP 1125, American Society for Testing and Materials, Philadelphia, 1992, p. 749.
[36] N.D. Evans, S.J. Zinkle, J. Bentley, in: I.M. Robertson et al. (Eds.), Microstructure of Irradiated Materials, MRS Symposium Proceedings, vol. 373, Materials Research Society, Pittsburgh, 1995, p. 419.

[37] Y.G. Chukalkin, V.V. Petrov, V.R. Shtirts, B.N. Goshchitskii, Phys. Status Solidi A 92 (1985) 347.
[38] K.E. Sickafus et al., J. Nucl. Mater. 219 (1995) 128.
[39] S.J. Zinkle, H. Matzke, to be published.
[40] A. Meftah et al., Mater. Sci. Forum 248–249 (1997) 53.